11TH INTERNATIONAL SYMPOSIUM ON PARTICLE IMAGE VELOCIMETRY –
PIV15 Santa Barbara, California, September 14-16, 2015

3D Turbulent Flow Measurements Combining V3V and Digital Inline Holographic PIV

Mostafa Toloui[1, 2], Wing Lai[3], Dan Troolin[3] and Jiarong Hong[1, 2]

[1] Department of Mechanical Engineering, University of Minnesota, Minneapolis, MN, USA

[2] Saint Anthony Falls Laboratory, University of Minnesota, Minneapolis, MN, USA

[3] Fluid Mechanics Division, TSI Incorporated, Shoreview, MN, USA
jhong@umn.edu

ABSTRACT

Wall-bounded turbulent flows generally cover a wide range of scales, which cannot be fully-resolved by any of the existing 3D PIV measurement techniques alone. In this study, two different 3D PIV measurement techniques, i.e. V3V and DIH-PIV, are combined to measure the 3D velocity fields above the rough surface composed of deformable cylinders. V3V measurement is implemented to capture significant flow structures up to integral scales of turbulence and the high resolution DIH-PIV is employed to capture fine near-wall flow structures down to the scale of few wall-unit. Specifically, the experiment is conducted in 1.2 m long test section of 50 mm square cross section, where the V3V system provides 1 mm vector spacing within a sampling volume of $60\times15\times40$ mm^3 (in the streamwise, wall-normal and spanwise directions). The DIH-PIV measurement volume (e.g. $0.5\times4\times0.5$ mm^3) is located right above a single cylindrical element within V3V sampling volume. The refractive index matching using NaI solution as working fluid is employed to minimize optical aberrations near the fluid-roughness interface. The resulted instantaneous flow fields display flow structures of a wide range of scales, from ~100 μm to ~ 1 cm. The averaged 3D velocity fields show a consistent trend of velocity distributions from both measurement techniques. Overall, the results show a great promise of combining DIH-PIV and V3V for a full-range scale quantification of wall-bounded turbulent flows.

1. INTRODUCTION

Wall-bounded turbulent flows are inherently three dimensional (3D), and cover a broad spectrum of flow structures, and the range of turbulent scales varying at different distances away from the wall. These features impose a significant challenge for implementing particle image velocimetry (PIV) to capture flow structures generated from the wall and their interaction with outer-layer flows. Although several 3D PIV techniques, including, e.g., tomographic PIV [1], volumetric three-component velocimetry (V3V) [2], and digital in-line holographic PIV (DIH-PIV) [3], etc., have been developed and employed for flow measurements, none of these technique alone is able to capture the full range of flow structures in wall-bounded turbulence. Specifically, tomographic PIV has been widely used for wall–bounded flow measurements. For example, Schröder et al. [4] employed tomographic PIV to study the evolution of coherent turbulent structures within the logarithmic region of turbulent boundary layer (TBL) in a sampling volume of $63 \times 15 \times 68$ mm^3 with the velocity spatial resolution of 2.5 mm × 2.5 mm × 2.5 mm in thestreamwise, wall-normal and spanwise directions, respectively, corresponding to $55 \times 55 \times 55$ wall units (WU). Ghaemi and Scarano [5] used tomographic PIV with improved velocity resolution of 1.7 mm× 0.9 mm× 1.7 mm (43×22×43 WU^3) to investigate the turbulent structure of high-amplitude pressure peaks within the TBL over a sampling volume of 16 × 6 × 24 mm^3. Using V3V, Ortiz-Dueñas *et al.* [6] investigated the effects of upstream cylindrical obstacles on TBL within 120 × 120 × 50 mm^3 volume of interest spanning 2.1 mm to 39.5 mm (52 WU to 1000 WU) in wall-normal direction. However, both of these techniques have been only restricted to quantifying larger scales flow motions (due to their limited spatial resolution) and the flows in the region above the inner layer of TBL. On the other hand, DIH-PIV have been successfully implemented for flow measurements the near wall region with significantly higher spatial resolution [7, 8]. For example, Sheng *et al.* [7] used DIH-PIV to study near wall coherent structures in a smooth wall channel flow within a volume of interest of 1.5 × 2.5 × 1.5 mm^3 starting at ~ 3.5 μm (0.2 WU) from the wall and with 51 μm × 136 μm × 17 μm (3×8×1 WU) resolution. Although, DIH-PIV provides significant increase in velocity spatial resolution and wall proximity measurement, it is currently restricted to much smaller measurement volume compared with those of tomographic PIV and V3V.

Recently, based on refractive-index-matching (RIM) technique, Hong *et al.* [9,10] and Talapatra *et al.* [8] have examined the turbulent flow structures within and above the roughness sublayer over a rough wall composed of pyramidal roughness elements using 2D PIV and DIH-PIV, respectively. Their results indicate the roughness elements generate unique coherent structures which can significantly alter the turbulent energy transport across a wide range of scales within and above the inner layer. These prior studies highlights the significance to obtain 3D characterization of the turbulent structures over a full range of scales that covers both near wall region and out-layer of the wall-bounded turbulent flows. Therefore, in the current study, we combine V3V and DIH-PIV to quantify the full range of flow structures in a rough-wall channel flow. Specifically, V3V is implemented to capture significant flow structures up to integral scales of turbulence, and the high resolution DIH-PIV is employed to capture fine near-wall flow structures down to micrometer scales. The detailed experimental methods and results are presented in the sections below.

2. EXPERIMENTAL SET-UP AND MEASURMENT TECHNIQUES:

2.1 REFRACTIVE INDEXMATCHING FLOW FACILITY

The experiments are conducted at separate times using both V3V and DIH-PIV over a rough wall in a refractive-index-matched (RIM) flow facility (Fig. 1). The facility is operated using sodium iodide solution with Reynolds number (based on the channel width), i.e. Re_h = 20000-60000. The test section is a 1.2 m long acrylic channel of 50 mm × 50 mm square cross section. It is designed with three windows located at upstream, middle section and downstream of the channel in order to facilitate the change of the upstream flow condition and rough surface conditions. In this experiment, the roughness is generated using a 200 mm (length) × 50 mm (width) stretch of tapered cylindrical elements, which is placed downstream of the channel (Fig. 2). Each roughness element is a cylinder of 1 mm in diameter and 3 mm in height made out of Polydimethylsiloxane (PDMS) polymer and spaced every 4 mm (center-to-center distance) in an aligned layout. The deformability of roughness is adjusted by controlling the mixing ratio of its two liquid components (cross-linking agent and SYLGARD 184 silicon elastomer), i.e. Young's modulus of PDMS solid samples range from 2.1 MPa to 0.15 MPa for weight mixing ratio of 2 to 20 [11]. Notably, under this range of deformability, the refractive index of the PDMS samples stays almost constant around 1.41 (< 0.01 change; [12]). To match the refractive index of the rough surface, the sodium iodine solution of 40 % by weight is employed as the working fluid during the experiments. For the current study, the flow facility is operated at Re_h = 26000, corresponding to a centerline velocity of U_c = 0.5 m s^{-1}, the channel width of 50 mm and the liquid viscosity equal to $\nu = \mu/\rho = 1.1 \times 10^{-6}$ m^2 s^{-1}.

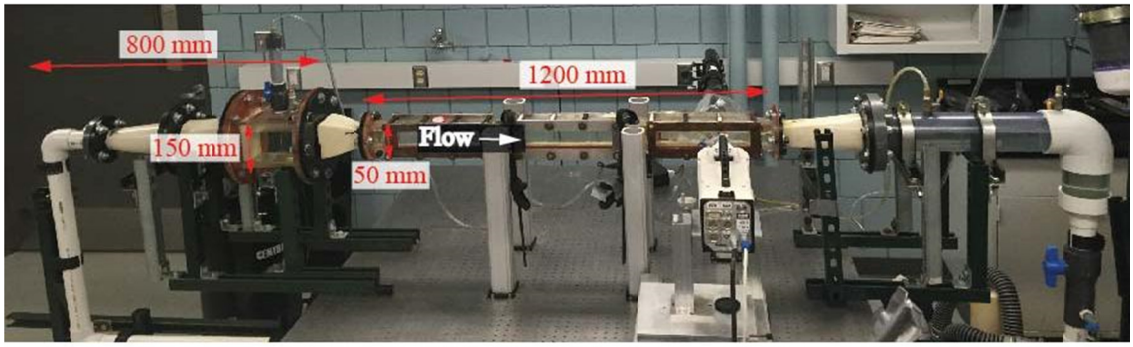

Figure 1 Refractive-index-matched flow facility operated with sodium iodide solution.

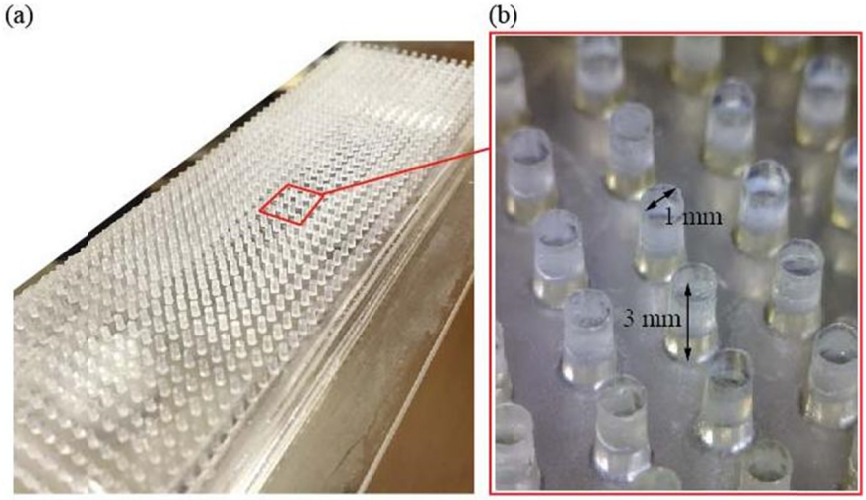

Figure 2 (a) The PDMS rough surface composed of an array of cylinders and (b) a close-up view of the PDMS cylindrical roughness elements.

2.2 V3V AND DIH-PIV

The separate experimental setups of V3V and DIH-PIV are constructed around the channel to perform flow diagnostics in the region of interest as shown in Figure 3. The V3V system, as illustrated in Figure 3a, consists of three CCD cameras, each containing 8 megapixels (3320 × 2496 pixels), and lenses of 85 mm focal length, providing a sampling volume of 60 mm × 15 mm × 40 mm (in the streamwise, wall-normal and spanwise directions) starting from 7 mm above the cylindrical elements (i.e. 10 mm from the bottom wall of the channel) with 5.5 µm/pixel (1 mm velocity spatial resolution). A double-pulsed Nd-YAG laser (wavelength of 532 nm, 10 ns pulse width) operating at 15 Hz and 200 mJ/pulse was used in the V3V system. The camera frames and laser pulses are triggered by a synchronizer running at 2.5 capture/s (each V3V capture consists of 6 separate images). The DIH-PIV system (shown in Figure 3b) uses a 12 mW HeNe laser (632 nm wavelength) as the coherent illumination source. The laser passes through a spatial filter and a lens assembly to generate a coherent collimated light beam, which penetrates horizontally into the channel and the resultant interference patterns form holograms that are recorded by a NAC Memrecam HX-5 high speed camera. A 10x EO-M-Plan infinity-corrected microscopic objective lens (NA = 0.45) is installed in front of the camera provides a 1 µm/pixel resolution for this DIH imaging system which is close to its Rayleigh diffraction limit (≈ 0.8 µm). The DIH imaging is conducted at 15µs exposure for 512 × 512 pixels imaging holograms at 20000 frames/s and captured with the focus plane set just on top of one cylindrical element (Figure 3c).

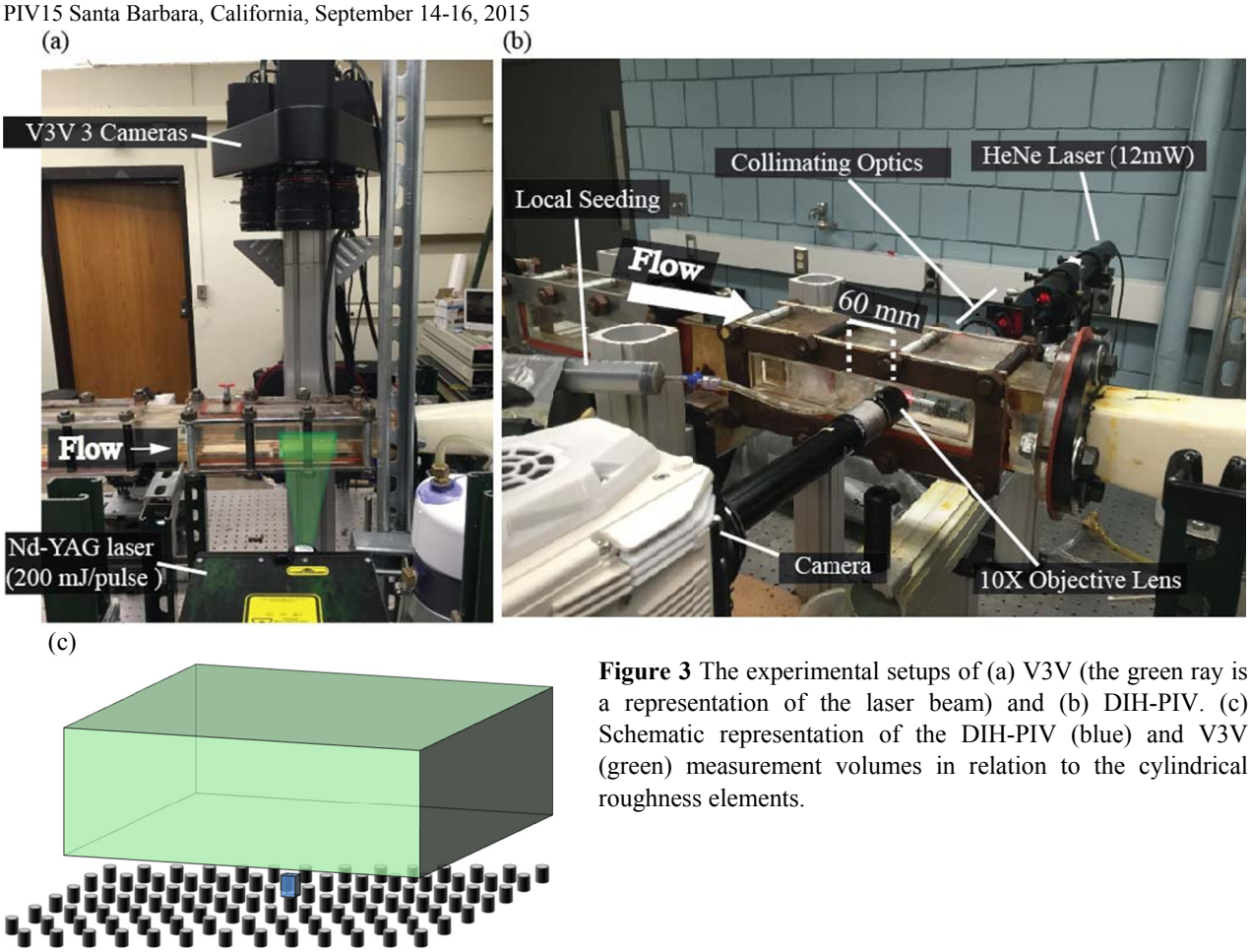

Figure 3 The experimental setups of (a) V3V (the green ray is a representation of the laser beam) and (b) DIH-PIV. (c) Schematic representation of the DIH-PIV (blue) and V3V (green) measurement volumes in relation to the cylindrical roughness elements.

The DIH-PIV sampling volume is located laterally in the center of the V3V volume of interest. This volume is locally seeded with 2 µm silver coated fused silica particles, in order to minimize background (out-of-focus) noise and achieve higher spatial resolution in the volume of interest. The local seeding is introduced through a set of five 200 µm holes located >300 hole diameters upstream of the FOV to ensure that the seeding causes no disturbance to the flow field in the sampling volume. The recorded particle holograms provide the 3D information corresponding to sampling volume of 0.5 × 4 × 0.5 mm^3 in the streamwise, wall-normal and spanwise directions for DIH-PIV measurements. The 3D information of particle fields are extracted from the recorded holograms using our in-house DIH-PIV processing algorithms (Toloui and Hong 2015 [13]) including several steps of 2D and 3D SNR-enhancements, automatic thresholding, 3D segmentation, iterative particle extraction and centroid calculation. The reconstructed 3D particle fields reveal that the holographic recordings in both cases cover 50 µm to 4 mm distance range from the bottom wall of the channel. The 3D velocity fields are then calculated implementing an open source 3D particle tracking program [14] on the consecutive tracer fields extracted through our IIPE algorithm.

3. RESULTS

Figure 4 presents two samples of instantaneous 3D velocity fields measured by V3V and DIH-PIV, respectively (the flow direction is into the page and to the right). The sample instantaneous velocity field over the large volume of 60 mm × 15 mm × 40 mm is obtained with the data closest to the wall occurring at 10 mm above the wall (i.e. 7 mm above the top of the cylinders) using V3V (Figure 4a). Similarly, a sample of 3D instantaneous velocity field measured through DIH-PIV over the small volume of 0.5 × 4 × 0.5 mm^3 starting 50 µm above the top of a single cylinder located laterally in the middle of V3V volume. For both high resolution (DIH-PIV) and large field of view (V3V) measurements, a planar slices show contours of the velocity magnitude with velocity vectors. In the larger volume, measured by V3V, the blue iso-surface represents regions of low streamwise velocity (0.68 U_c) and the green iso-surfaces represent vorticity magnitude (31 s^{-1}). Of note in the plot is the low-speed streak present near the wall, and the resulting vorticity generated. Complex looped vortical

structures appear straddling the low-speed streak and interacting as the streak is convected downstream. The sample instantaneous velocity field measured using DIH-PIV within the smaller volume also shows an increase in velocity magnitude with height as well as a small vortical flow structure, marking a part of the recirculation zone on top of the cylindrical roughness.

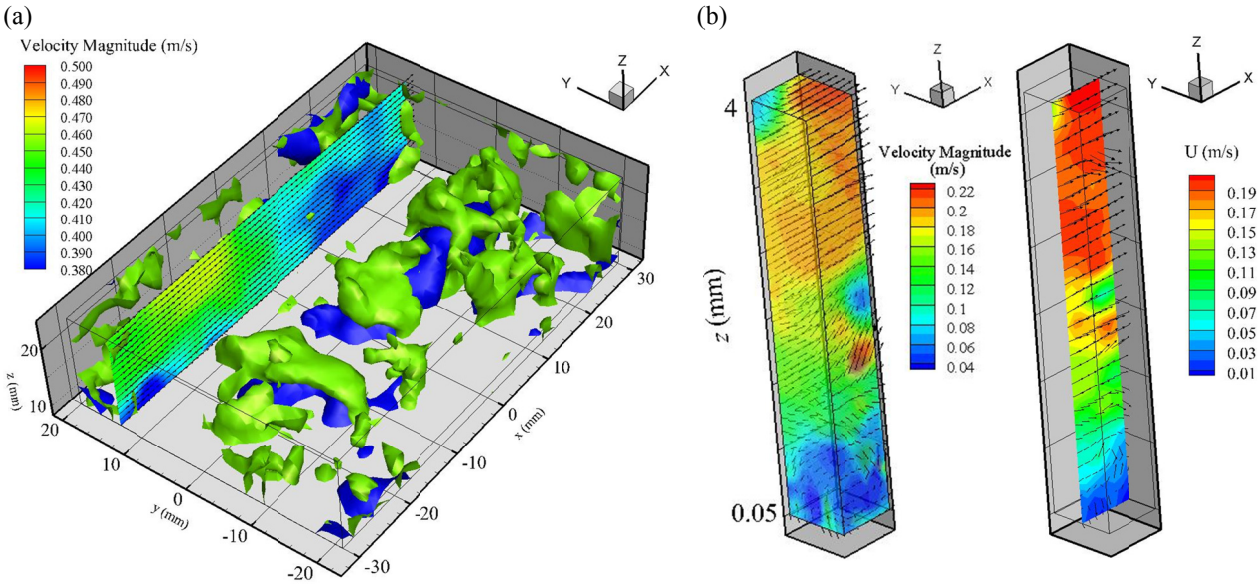

Figure 4 A sample of instantaneous 3D velocity vector fields from: (a) V3V within 60 × 15 × 40 mm^3 measurement volume and 1 mm/vector resolution (the blue isosurface represents regions of low streamwise velocity (0.68 U_c) and the green isosurfaces represent vorticity magnitude of 31 s^{-1}) and (b) DIH-PIV within 0.5 × 4 × 0.5 mm^3 measurement volume and 100 µm/vector resolution.

The 3D average velocity fields are calculated for both measurement volumes using 250 and 300 instantaneous velocity field samples for V3V and DIH-PIV measurements, respectively. The ensemble averaged 3D velocity fields for both techniques are presented in Figure 5. The flow is out of the page and to the right. The slices contain color contours representing the streamwise velocity, overlaid with velocity vectors. The plot shows a continuous increase of velocity as z (wall-normal) increases i.e. closer to the core (red in V3V) of the channel flow, and the slower moving boundary layer regions (blue). The offset between two measurements volumes covers a region of 7 mm to 10 mm away from the wall (or 4 mm to 7 mm above the cylindrical roughness element), and this explains ~ >0.1 m/s difference between the minimum value of velocity measured by V3V and the maximum measured by DIH-PIV.

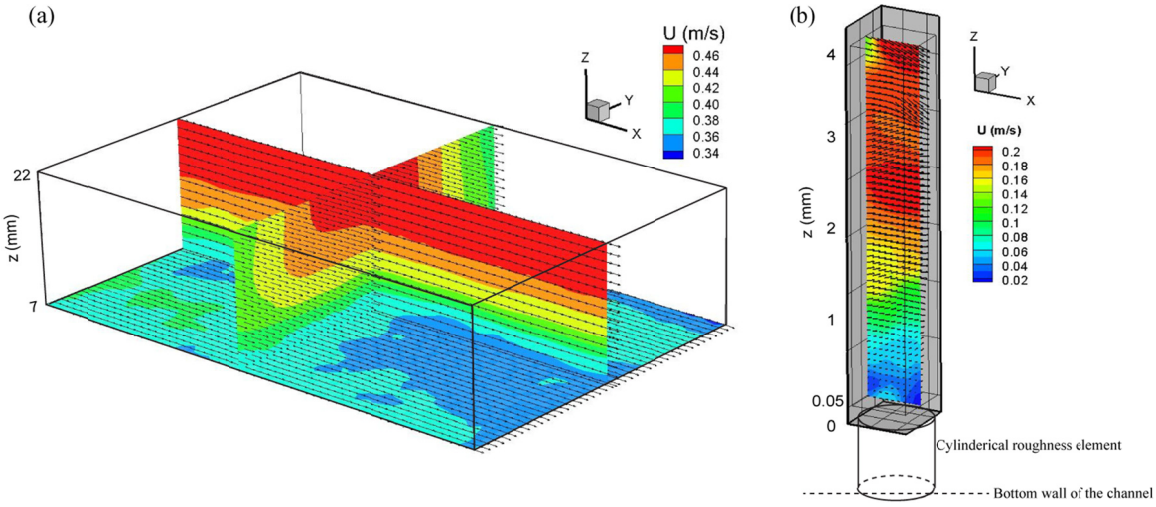

Figure 5 The measured mean velocity vector fields superimposed with the contours of streamwise velocity magnitude using: (a) V3V within 60 × 15 × 40 mm^3 measurement volume and (b) DIH-PIV within 0.5 × 4 × 0.5 mm^3 measurement volume.

As a future step in this study, in order to characterize the turbulent flow structures and turbulent statistics within and above the roughness sublayer, the experiments will be repeated within an overlapping measurement volume for both high resolution (using DIH-PIV) and large field of view (V3V). Specifically, the sampling volume of 1 mm × 4 mm × 1 mm for DIH-PIV will be set in the middle of V3V measurement that covers 50 mm × 20 mm × 50 mm volume, and both volumes will start from the bottom wall of the channel. The measurements will be conducted over rough walls with similar geometrical features but various deformability levels (Young's modulus ranging from 0.15 MPa to 2.1 MPa). These experiments will provide insights into the effect of roughness deformability on near-wall coherent structures and turbulent energy transport within and above the roughness sublayer.

REFERENCES

[1] Elsinga, G. E. (2008). Tomographic particle image velocimetry and its application to turbulent boundary layers (Doctoral dissertation, TU Delft, Delft University of Technology).

[2] Lai, W., Pan, G., Menon, R., Troolin, D., Graff, E., Gharib, M., & Pereira, F. (2008, July). Volumetric three-component velocimetry: a new tool for 3d flow measurement. In *Proceedings of the 14th international symposium on applications of laser techniques to fluid mechanics. Lisbon, Portugal*.

[3] Katz, J., & Sheng, J. (2010). Applications of holography in fluid mechanics and particle dynamics. *Annual Review of Fluid Mechanics*, *42*, 531-555.

[4] Schröder, A., Geisler, R., Staack, K. É. A. A., Elsinga, G. E., Scarano, F., Wieneke, B., ... & Westerweel, J. (2011). Eulerian and Lagrangian views of a turbulent boundary layer flow using time-resolved tomographic PIV.*Experiments in fluids*, *50*(4), 1071-1091.

[5] Ghaemi, S., & Scarano, F. (2013). Turbulent structure of high-amplitude pressure peaks within the turbulent boundary layer. *Journal of Fluid Mechanics*,*735*, 381-426.

[6] Ortiz-Dueñas, C., Ryan, M. D., & Longmire, E. K. (2011). Modification of turbulent boundary layer structure using immersed wall-mounted cylinders. *Proceedings Turbulence and Shear Flow Phenomena VII*.

[7] Sheng, J., Malkiel, E., & Katz, J. (2008). Using digital holographic microscopy for simultaneous measurements of 3D near wall velocity and wall shear stress in a turbulent boundary layer. *Experiments in fluids*, *45*(6), 1023-1035.

[8] Talapatra, S., & Katz, J. (2013). Three-dimensional velocity measurements in a roughness sublayer using microscopic digital in-line holography and optical index matching. *Measurement Science and Technology*, *24*(2), 024004.

[9] Hong, J., Katz, J., & Schultz, M. P. (2011). Near-wall turbulence statistics and flow structures over three-dimensional roughness in a turbulent channel flow.*Journal of Fluid Mechanics*, *667*, 1-37.

[10] Hong, J., Katz, J., Meneveau, C., & Schultz, M. P. (2012). Coherent structures and associated subgrid-scale energy transfer in a rough-wall turbulent channel flow. *Journal of Fluid Mechanics*, *712*, 92-128.

[11] Liu, M., & Chen, Q. (2007). Characterization study of bonded and unbonded polydimethylsiloxane aimed for bio-micro-electromechanical systems-related applications. *Journal of Micro/Nanolithography, MEMS, and MOEMS*, *6*(2), 023008-023008.

[12] Qiu, W. (2012). PDMS Based Waveguides for Microfluidics and EOCB (Doctoral dissertation, Zhejiang University).

[13] Toloui, M. and Hong J. (2015) "High Fidelity Digital Inline Holographic Method for 3D Flow Measurements", *Optics Express* (2015) (submitted).

[14] Crocker, J. C., & Grier, D. G. (1996). Methods of digital video microscopy for colloidal studies. *Journal of colloid and interface science*, *179*(1), 298-310.